



Pressure drop measurements and hydrodynamic model description of SiC foam composites decorated with SiC nanofiber

David Edouard^{a,1,*}, Svetlana Ivanova^{a,1}, Maxime Lacroix^{a,1}, Estelle Vanhaecke^{a,1}, Charlotte Pham^b, Cuong Pham-Huu^{a,1}

^a Laboratoire des Matériaux, Surfaces et Procédés pour la Catalyse (LMSPC), ECPM-Université Louis Pasteur, 25 rue Becquerel, 67087 Strasbourg Cedex 02, France

^b SiCat Technical Center, 1 rue du Broetch, 67700 Otterswiller, France

ARTICLE INFO

Article history:

Available online 21 July 2008

Keywords:

SiC foam composite
Nanofiber
Pressure drop
Hydrodynamic model
Specific surface area
Catalysis

ABSTRACT

During the last decade there has been a growing interest in catalytic reactor engineering based on structured catalytic beds. Compared to traditional packed bed reactors, structured catalytic beds provide improved hydrodynamics and catalytic performance. In this context, silicon carbide (SiC) foam materials seems to be a good candidate for use as catalyst support due to their high geometrical surface area (m^{-1}) and open porosity leading to low pressure drop. However, foam structures have a relatively low specific surface area (m^2/g) for performing good anchorage and dispersion of the active phase which is one of the crucial points in catalysis. This study proposes a new type of material which combined the advantage of foam (high porosity) with nanofiber of SiC (high specific surface (m^2/g)). The knowledge of pressure drop characteristics of foam with nanofiber is necessary for the future process design. However, due to the complexity of the geometric shape of new foam materials, up to date, no general relationship exists for the calculation of the pressure drop through different foam matrix and generally, empirical equation with modified parameters of the Ergun's equation were needed to fit the data. This study show that a simple model can be used for the prediction of the pressure drop in the SiC foam with nanofiber through Ergun's equation without using any fitting in order to reconcile experimental data with theory.

© 2008 Elsevier B.V. All rights reserved.

1. Introduction

The use of porous structures with high external surface area represents an important breakthrough in industrial catalytic applications. The main advantage of using these porous structures is the high contact surface (geometrical surface area (m^{-1})) between the fluid and solid phase and also the low pressure drop along the catalyst bed. One eminent example of classical catalytic bed is a packed bed, which is frequently utilized as catalyst support and thermal energy storage device [1]. However, due to its low porosity (in the range of 0.3–0.6), packed bed induces an important pressure drop at high flow which is detrimental for the operating system, especially when high space velocity is required for maintaining acceptable selectivity by phasing-out the unwanted secondary reactions. The main drawbacks of classical

catalytic beds could be summarized as (i) high pressure drop through the catalytic bed due to the high gaseous space velocity, (ii) limited heat and mass transfers, (iii) flow maldistribution leading to loss of selectivity, and (iv) susceptibility to fouling by dust [2].

During the last decade there has been a growing interest in catalytic reactor engineering based on structured catalytic beds [3,4]. The idea of moving from the traditional packed-bed, e.g. extrudates, pellets, to the structured bed, i.e. monolith, wire or foam either made of stainless steel or ceramic, is become more and more popular. Foam matrixes have been recently introduced to overcome some of the above shortcomings dealing with the use of the packed bed. This new medium has as a highly permeable structure with high porosity (0.60–0.95), which enables a considerably reduction of the pressure drop along the catalyst bed even at high gaseous space velocity. However, foam structures have a relatively low specific surface area (m^2/g), due to the methods of preparation which requiring usually high temperatures operation [5,6], for performing good anchorage and dispersion of the active phase.

* Corresponding author. Tel.: +33 0390242676.

E-mail address: edouard@ecpm.u-strasbg.fr (D. Edouard).

¹ Member of the European Laboratory for Catalysis and Surface Science (ELCASS).

Nomenclature

a	window or pore diameter (μm)
a_c	BET or external specific surface (m^{-1})
d_p	particle diameter (μm)
d_{peq}	equivalent diameter (μm)
d_s	strut diameter (μm)
$E_{1,2}$	Ergun constants
k_1	permeability coefficient (m^2)
k_2	inertial coefficient (m^{-1})
L	length of foam (m)
ΔP	pressure drop (Pa)
u	fluid velocity (m s^{-1})

Greek symbols

ε	porosity
ρ_g	apparent density (g/l)
ρ_s	strut bulk density (g/l)

SiC foam present medium specific surface but still low compared to classical packing bed (i.e. extrudates) [7]. In this context, the addition of the nanoscopic size SiC nanofibers [8] could significantly increases the specific surface area of the initial support (SiC foam) for subsequent better active phase dispersion without introducing new drawbacks. In addition to the specific surface area, the pressure drop is another very important parameter for the characterization of catalytic supports employed in industrial applications. The knowledge of pressure drop induced by these support is essential for successful design and operation of high performance industrial systems. Introducing nanoscopic material into macroscopic host matrix generally develop pressure drop due to the narrowing of the flowing space along the composite. In this context, the aim of this paper is to examine the effect of addition of the SiC nanofibers in the prediction of bed permeability based on previous model [9].

2. Experimental

2.1. Composite preparation

The SiC foam synthesized according to the gas–solid reaction [10,11] with an average cell size of $1900 \mu\text{m}$ was impregnated with an aqueous solution of $\text{Ni}(\text{NO}_3)_2 \cdot 6\text{H}_2\text{O}$ (Strem Chemicals). The nickel loading was set to be 1 wt%. The solid was oven-dried at 100°C for 2 h and calcined in air at 350°C . The reduction was carried out *in situ* in flowing hydrogen at 400°C for 1 h. The hydrogen was replaced by a mixture of $\text{C}_2\text{H}_6/\text{H}_2$ (60/40 ml/ml per minute) and the reaction temperature was increased from 400 to 680°C (heating rate of $20^\circ\text{C min}^{-1}$) [12]. A network of carbon nanofibers was generated under these conditions. The synthesis was lasted for 3 h and the reactor was cooled down to room temperature under the reactants mixture. The reactor was flushed with helium for 30 min before discharging the solid from the reactor.

SiC nanofibers were synthesized by reaction between the carbon nanofibers (CNFs) with the SiO vapours under argon atmosphere at 1300°C for 4 h in an electrical oven. The transformation of C to SiC was accompanied by a consecutive release of CO which was actively flushed out from the reaction zone by the argon flow and thus, shifting the reaction equilibrium

towards the formation of SiC. The relatively low synthesis temperature allows the conservation of the specific surface area of the produced SiC material (β -SiC) unlikely the high temperature synthesis where only α -SiC with very low specific surface area, i.e. $0.1\text{--}1 \text{ m}^2/\text{g}$ is obtained [13,14]. After synthesis the ceramic composite was calcined in air at 600°C for 2 h in order to remove the residual carbon in its matrix.

2.2. Characterization techniques

The specific surface area was determined by nitrogen adsorption–desorption at 77 K by BET method on a Micromeritics sorptometer Tri Star 3000. Before adsorption the samples were outgased at 300°C for 4 h in order to desorb water on the surface and in the pore volume.

The morphology of SiC foam sample was investigated by means of a scanning electron microscopy (SEM) and carried out on a Jeol JSM-6700F working at 3 kV accelerated voltage, equipped with a CCD camera. The samples was previously coated with carbon and then deposited on a standard holder for observation. The optical images presented in Fig. 1 have been taken with an optical microscope Digital Blue equipped with a numerical camera. From this figure, the main morphological characteristics of foams were examined (i.e. the diameters of the windows (or pores diameter, a) and the thickness of the struts (d_s)).

Another important parameter of these structures is the foam porosity (ε) which is the volume available for the fluids flow through the open-cell structure. Generally in the literature, ε can be calculated on the basis of mass and volume measurements using the expression $\varepsilon = 1 - \rho_g/\rho_s$, where ρ_g is the foam apparent density and ρ_s is the materials density of the struts. The material strut bulk density (ρ_s) and internal porosity can be obtained by different porous distribution techniques (mercury intrusion [9], water picnometer [15], He multipycnometer [16]). In this work, the strut bulk density (ρ_s) was determined by mercury intrusion.

Finally, for each samples of SiC (extrudates, foam and foam with SiC nanofibers) studies in this work, the main morphological characteristics of the sample and the corresponding specific surface area (m^2/g) measured by BET method are summarized in Table 1.

2.3. Pressure drop set-up

Experimental pressure drop (ΔP) across each sample was measured using the apparatus schematized in Fig. 2 and presented

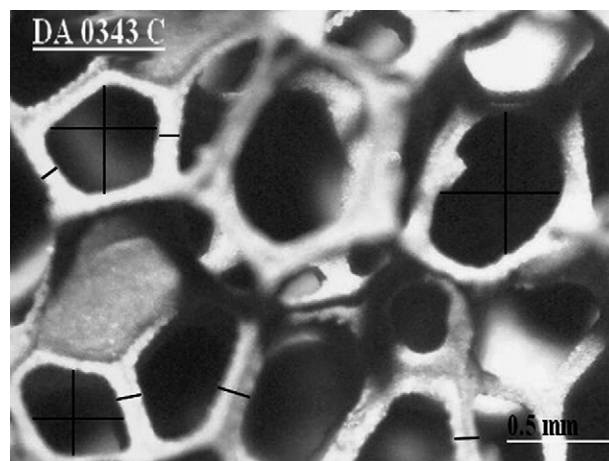


Fig. 1. Optical pictures of $1900 \mu\text{m}$ SiC foams showing the detail morphology and connection structure of the material.

Table 1
Support characteristics

Support characteristics	SiC extrudates given by SiCat	SiC foam	SiC foam with 5 wt% NF	SiC foam with 39 wt% NF
Cell diameter		1900 μm	1900 μm	1900 μm
Apparent mass, ρ_{app}	770 g/l	103 g/l	107.5 g/l	169 g/l
Open porosity, ε	0.38	0.94	0.937	0.902
Equivalent extrudates diameter ^a or calculated strut diameter or equivalent calculated strut diameter ^b	3 mm ^a	157 μm	161 μm^b	211 μm^b
Calculated geometrical specific surface area, ac_g	1461 m ⁻¹	1530 m ⁻¹	1560 m ⁻¹	1852 m ⁻¹
Specific surface area, BET	34 m ² /g	10 m ² /g	19 m ² /g	50 m ² /g

in previous work (see for detail [9]). The diameter of the tube in the set-up for measuring the pressure drop is 25.4 mm. It is the low limit to neglect wall effects. Gas velocity is measured with anemometer Testo 435-1 equipped with hot wire probe (0–20 m s⁻¹). Pressure drop was measured with differential pressure sensor (Keller Druckmesstechnik PD-41 (0–200 mbar)). Pressure drop was measured on 0.04 m long foams varying the gas velocity in the 0–5 m s⁻¹ range.

2.4. Model of pressure drop

The Ergun's equation (1) is a well-known relation for pressure drop prediction for any kind of packed bed [17]:

$$\frac{\Delta P}{L} = E_1 \frac{\mu(1-\varepsilon)^2 u_f}{\varepsilon^3 d_p^2} + E_2 \frac{\rho(1-\varepsilon) u_f^2}{\varepsilon^3 d_p} = \frac{1}{k_1} \times \mu u_f + k_2 \times \rho u_f^2 \quad (1)$$

where ($\Delta P/L$) is the pressure drop per unit length, E_1 and E_2 are Ergun constants (respectively 150 and 1.75) and u_f is the superficial velocity. The major problem in the foam pressure drop estimation is to reliably define structural properties of the cellular medium to

replace the particle diameter (d_p) in Eq. (1). Many approaches use directly the size of the window (or pore diameter) or strut diameter as the characteristic of the foam. But in order to give accurate estimation of the pressure drop Ergun's coefficient E_1 and E_2 need to be optimized [15,16,18,19]. In model developed by Lacroix et al. [9] a direct analogy between foams and a virtual spherical packed bed is designed from the cubic lattice model in order to present the same porosity and exchange specific surface [m²/m³] as the original foam. A simple geometrical consideration based on the cubic cell model [9] gives the relationship between strut and particle equivalent diameter (Eq. (2)) for a porous medium (see [9] for detailed demonstration):

$$d_{\text{peq}} = \frac{3}{2} d_s \quad \text{with} \quad d_s = \frac{a[(4/3\pi)(1-\varepsilon)]^{1/2}}{1 - [(4/3\pi)(1-\varepsilon)]^{1/2}} \quad (2)$$

The specific geometrical surface area (m⁻¹) obtained by this approaches is then given by:

$$ac_g = \frac{4}{d_s} (1-\varepsilon) \quad (3)$$

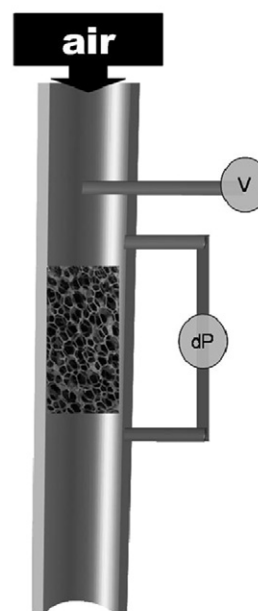
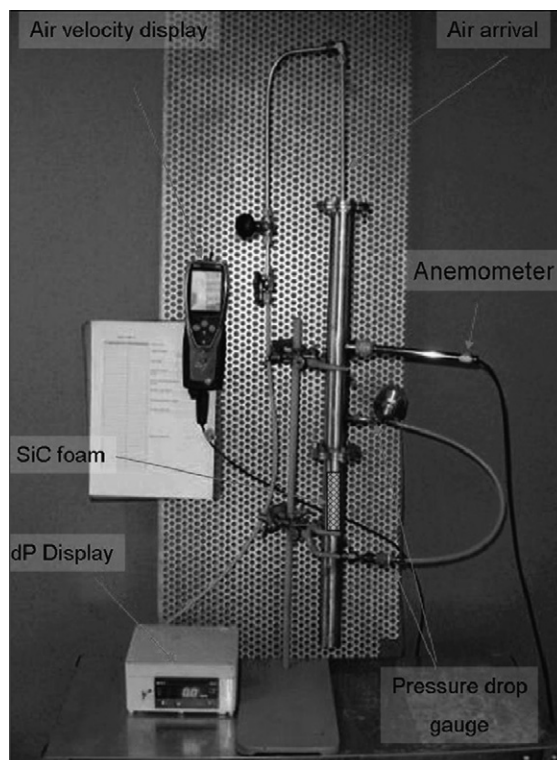


Fig. 2. Apparatus for pressure drop measurements.

Replacing d_p by d_{peq} in Ergun's equation allows to predict quite well the pressure drop through SiC cellular foams with different pore sizes and different porosities [9]. This model could be also applied to foams made of different materials (Al_2O_3 , Ni, Cu, ...).

3. Results and discussion

In Fig. 1 a representative SEM micrographs of the SiC foam with different magnifications are presented. High resolution SEM observation (Fig. 1B) clearly evidence the presence of porosity within the material strut. The porosity was attributed to the gas–solid reaction which involve the formation of gaseous CO which induce pores formation inside the material wall. The highly porous microstructure of the as-synthesized SiC foam was in good agreement with the medium specific surface area obtained by N_2 adsorption at liquide nitrogen temperature, i.e. $10\text{ m}^2/\text{g}$.

The formation of the carbon nanofibers (CNFs) on the SiC foam surface induces a significant improvement of the specific surface area from 10 to $60\text{ m}^2/\text{g}$. Taken into account the fact that the specific surface area of the SiC host structure was not modified during the CNF growth process the real specific surface area of the as-synthesized CNF was around $150\text{--}200\text{ m}^2/\text{g}$ which is fall within the range of bulk carbon nanofibers reported in the literature. The CNF anchorage was extremely strong as no matter loss has been observed after sonication of the sample for 30 min. The high mechanical anchorage of the CNF onto the SiC host structure was attributed to the growth mechanism where part of the CNF deeply penetrate the host matrix.

The as-synthesized CNFs/SiC foam composite was further carburized and the specific surface area was slowly decreased after carburization process to $50\text{ m}^2/\text{g}$ (Table 1). From Table 1, it could be seen that the specific surface area (m^2/g) increased with the nanofibers deposition as well as the apparent masse while the porosity of foam decreased. According to the obtained results for the classical systems, i.e. extrudate or grains in packed-bed, the pressure drop is quite important and becomes higher as the gas velocity increases, as seen in Fig. 3. At high gas velocity, for example 3 m s^{-1} , pressure drop was near $1 \times 10^4\text{ Pa/m}$ of foam, whereas it was higher than 8×10^4 in the case of extrudates. Richardson et al. [16] quote a factor of 10 between the pressure

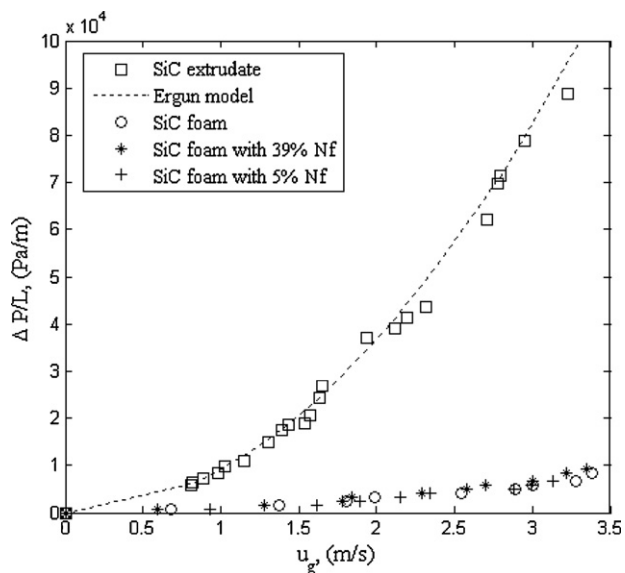


Fig. 3. Pressure drop as a function of linear space gas velocity on the starting SiC foam and extrudates and the SiC-NF/SiC foam composite with different amounts of nanofibers.

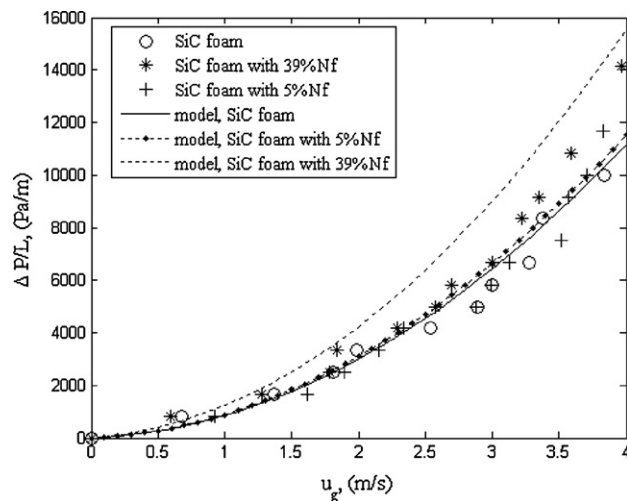


Fig. 4. Comparison between experimental data and simulated pressure drop of the starting SiC foam and the SiC-NF/SiC foam composite as a function of linear space velocity.

drop recorded for the foam-type supports and spherical particles fixed bed. This figure shows clearly that even with a high specific surface area (BET measurements shown in Table 1), the pressure drops through the solid SiC foams with the SiC nanofibers (SiC-NF/SiC) are lower than those of the packed bed of extrudates. And thus confirming that the composite constituted by nanofibers supported on foams are good candidates as a support for catalytic reactions with short contact times (i.e. high reactant flows).

The introducing of nanoscopic material into macroscopic host matrix of foams has hardly influence on the pressure drop as shown in Fig. 4. The obtained results are similar. To explain this phenomenon, we estimated the pressure drop on the SiC-NF/SiC foam composite given by the cubic cell model developed by Lacroix et al. [9] that show a good agreement between estimated pressure drops and experimental data (Fig. 4). In the pressure drop simulations, cell diameter is constant and only foam apparent density and thus porosity change. As seen from Table 1, the porosity decreases with the nanofibers deposition and following Eq. (2), the calculated equivalent strut diameter increases and induced from Ergun's equation only a low increasing of pressure drop.

To verify the influence of the nanofibers on the strut diameter the microscopic observations have been carried out (Fig. 5). SEM image (Fig. 5D) shows a complete coverage of the SiC foam surface by a dense web network constituted by entangled SiC nanofibers. Thus for modeling the pressure drop on foam cover with nanofibers, it is sufficient to consider that the nanofibers can be homogeneously distributed along the struts and that only knowledge of apparent density (and thus porosity) is necessary to estimate the pressure drop induced by SiC foams covered by nanofibers and by this approach will be well adapted for the future process design.

However in reality, the matter (nanofibers) was not homogeneously deposited on the surface of the strut, the material surface present a certain roughness (Fig. 5B and C). Buciuman and Kraushaar-Czarnetzki [15] used the BET specific surface area (m^2/g) multiplied by the apparent densities (ρ_g) of the foams to compare the geometrical specific surface area (m^{-1}). Authors obtained in first approximation a good agreement between the model calculations and experimental data in the case of China porcelain foam, but a large deviation was observed with the same correlation for alumina-mullite foam. In this case, the foam

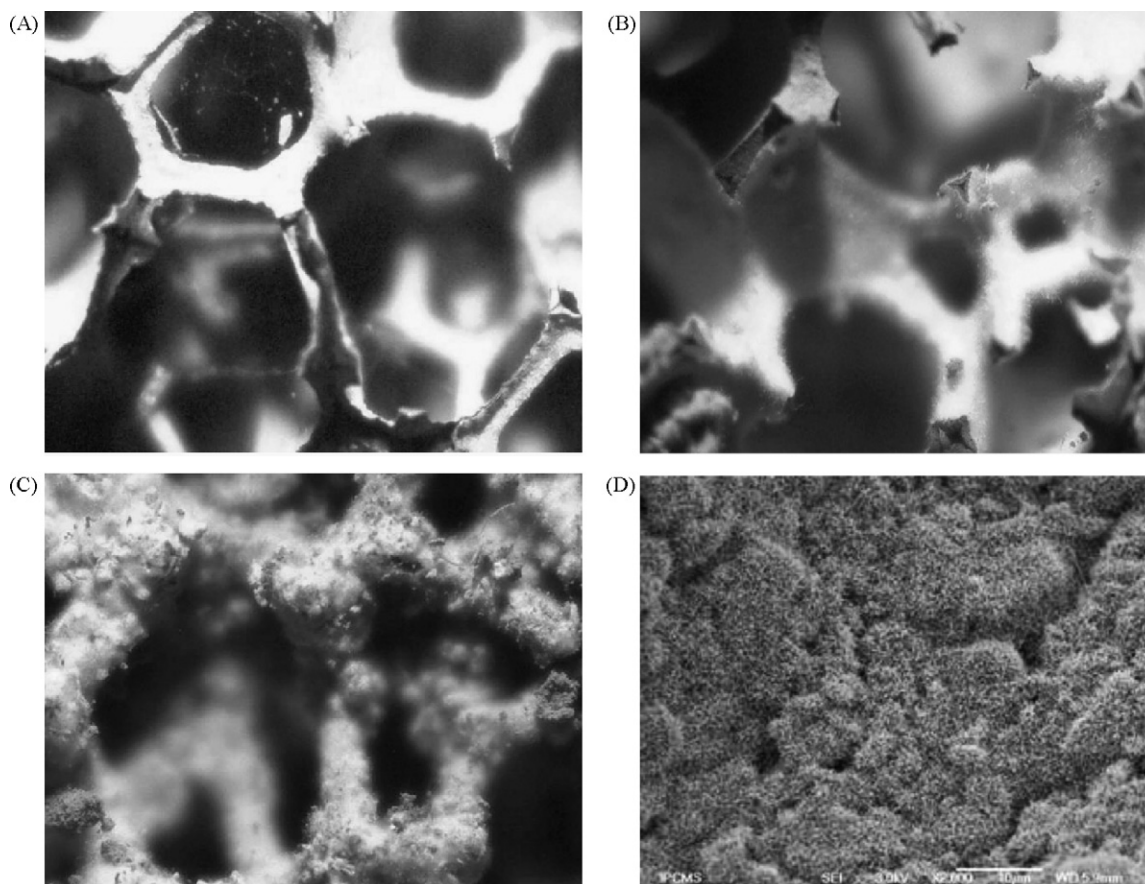


Fig. 5. (A) Optical images of SiC strut, (B) optical images of 5 wt% NFSiC/SiC struts, (C) optical images of 39 wt% NFSiC/SiC struts, and (D) SEM micrograph of SiC nanofibers on SiC surface (39 wt% NFSiC/SiC sample).

skeleton was formed upon diffusive sintering of the particles, thus resulting in more rough struts. The BET measurement for alumina-mullite foam is near to $0.02 \text{ m}^2/\text{g}$, which implies a low surface roughness and by this a small difference between the experimental and calculated specific surface area. The hollow struts are accessible for gas adsorption in BET measurements and in this case the geometrical model used to calculate the specific surface area takes into account only the spatial arrangement and dimensions of the struts rather than their specific surface area characteristics. The

difference between the experimental and calculated specific surface area can give direct information of the effects of surface roughness of foams (see for detail [15]). In the same way, from Fig. 6 it could be seen that the geometrical surface area (m^{-1}) obtained by the model of Lacroix et al. [9] is more close to the data for China porcelain foam presented by Buciuman and Kraushaar-Czarnetzki [15]. For SiC foam with nanofiber the difference is more important and show that the struts become rougher (see Fig. 5). This effect of surface roughness lead to envisaging that this catalytic support will be good structures for performing good anchorage and dispersion of the active phase necessary for obtained for example a good selectivity and will be subject of a future work.

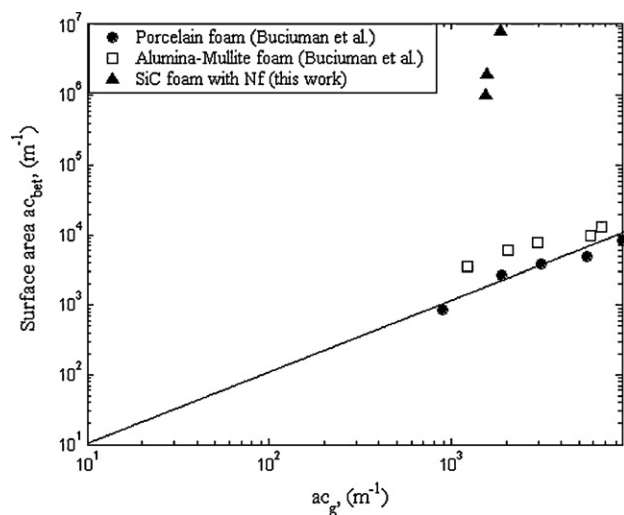


Fig. 6. Parity diagram of experimental surface area versus theoretical value.

4. Conclusion

The deposition of SiC nanofibers over a macroscopic solid SiC foam surface highly increases the specific surface area of the final composite and successfully combines the macroscopic shape and nanoscopic properties. As far as one knows this will change for sure the properties of the support assuring better dispersion of any active phase. A simple pressure drop model using the standard Ergun's equation and based on a cubic lattice approach of the foam structure is used [9]. This model allows predicting experimental data on the foam structure with or without nanofiber. Experimental data and estimated pressure drop show that introducing of nanoscopic material into macroscopic host matrix of foams has not important influence to the pressure drop. Work is ongoing to predict the hydrodynamic behavior of the final composite in a

complex exothermic trickle flow reaction, i.e. Fischer Tropsch synthesis or partial oxidation reactions.

Acknowledgements

SiCat is gratefully acknowledged for providing SiC foam samples and also for helpful discussions and advices.

References

- [1] F.W. Schmidt, A.J. Willmott, Thermal Energy Storage and Regeneration, McGraw-Hill, New York, 1981, p. 178.
- [2] S. Ivanova, B. Louis, B. Madani, J.P. Tessonier, M.J. Ledoux, C. Pham-Huu, J. Phys. Chem. C 111 (2007) 4368.
- [3] G. Groppi, E. Tronconi, Design of novel monolith catalyst supports for gas/solid reactions with heat exchange, Chem. Eng. Sci. 55 (12) (2000) 2161–2171.
- [4] L. Giani, G. Groppi, et al., Mass-transfer characterization of metallic foams as supports for structured catalysts, Ind. Eng. Chem. Res. 44 (2005) 4993–5002.
- [5] L.J. Gibson, M.F. Ashby, Cellular Solids, Structure and Properties, Second edition, Cambridge Solid State Science Series, Cambridge, 2001, p. 235.
- [6] O.O. Omatete, M.A. Janney, S.D. Nunn, J. Eur. Ceram. Soc. 17 (1997) 407.
- [7] R. Moene, Ph.D. Thesis, Delft, 1995.
- [8] E. Vanhaecke, S. Ivanova, G. Winé, D. Edouard, P. Nguyen, Ch. Pham, C. Pham-Huu, Journal of Materials Chemistry, in press.
- [9] M. Lacroix, P. Nguyen, D. Schweich, C. Pham Huu, S. Savin-Poncet, D. Edouard, Chem. Eng. Sci. 62 (2007) 3259.
- [10] M.J. Ledoux, J. Guille, S. Hantzer, D. Dubots, US 4914070, assigned to Pechiney 1990.
- [11] M.J. Ledoux, C. Pham-Huu, Catal. Today 15 (1992) 263.
- [12] R. Vieira, M.J. Ledoux, C. Pham-Huu, Appl. Catal. A: Gen. 274 (2004) 1.
- [13] Y.-J. Hao, G.-Q. Jin, X.-D. Han, X.-Y. Guo, Mater. Lett. 60 (2006) 1334.
- [14] Y.-J. Hao, J.B. Wagner, D.S. Su, G.-Q. Jin, X.-Y. Guo, Nanotechnology 17 (2006) 2870.
- [15] F.C. Buciuman, B. Kraushaar-Czarnetzki, Ind. Eng. Chem. Res. 42 (2003) 1863.
- [16] J.T. Richardson, Y. Peng, D. Remue, Appl. Catal. A: Gen. 204 (2000) 19.
- [17] S. Ergun, Chem. Eng. Prog. 48 (1952) 89.
- [18] J.F. Liu, W.T. Wu, W.C. Chiu, W.H. Hsieh, Exp. Therm. Fluid Sci. 30 (2006) 329.
- [19] D.M. Murilo Innocentini, V.R. Salvini, A. Macebo, V.C. Pandolfelli, Mater. Res. 2 (1999) 283.